

**Transverse Equilibria and Luminosity Enhancement
in Linear Collider Beam-Beam Collisions***

J.B. Rosenzweig
*UCLA Department of Physics
405 Hilgard Ave.
Los Angeles, CA 90024*

Pisin Chen
*Stanford Linear Accelerator Center
Stanford University, Stanford, California 94309*

Abstract

It has been observed in simulations of the beam-beam interaction in linear colliders that a near equilibrium pinched state of the colliding beams develops when the disruption parameter is large ($D \gg 1$) [1]. In this state the beam transverse density distributions are peaked at center, with long tails. We present here an analytical model of the Maxwell-Vlasov equilibrium approached by the beams, that of a generalized Bennett pinch [2] which develops through collisionless damping due to the strong nonlinearity of the beam-beam interaction. In order to calculate the equilibrium pinched beam size, an estimation of the rms emittance growth is made which takes into account the effects of the initial linear rise of the focusing forces, and of phase space mismatch during the beam-beam collision. This pinched beam size is used to derive the luminosity enhancement factors whose scaling as a function of D and thermal factor $A = \sigma_z / \beta^*$ is in agreement with the simulation results, and explain the previously noted cubic relationship between round and flat beam enhancement factors. The implications for calculation of differential luminosity, beamstrahlung spectra, and associated coherent beam-beam radiation effects, are discussed.

Submitted to *Physical Review E*.

* This work supported with partial support from Department of Energy DE-AC03-76SF00515, DE-FG03-90ER40796 and DE-FG03-92ER40693, Texas National Research Laboratory grant FCFY9308 and the Sloan Foundation grant BR-3225.

I. Introduction

The calculation of the luminosity enhancement of electron-positron linear collider beam-beam collisions due to the mutual strong focusing, or disruption, of the beams has been traditionally calculated[1] by use of particle-in-cell computer codes. These numerical calculations solve for electromagnetic fields and the motion of the particles which generate these fields self-consistently. The emergence of near equilibrium "pinch-confined" transverse beam profiles in the limit that the disruption parameter

$$D_{x,y} \equiv \frac{2Nr_c\sigma_z}{\gamma(\sigma_x + \sigma_y)\sigma_{x,y}}, \quad (1)$$

is much greater than unity has been noted; in this regime the beam particles undergo multiple betatron oscillations during the collision. In the above expression $\sigma_{x,y}$ are the transverse rms beam sizes, σ_z is the rms bunch length, N is the number of particles per bunch, and γ is the beam particle energy normalized to the rest energy, and the spatial beam distributions are assumed to be Gaussians. It is proposed here that these near equilibrium states are approached through collisionless damping due to mixing and filamentation in phase space, in analogy to a similar phenomena found in self-focusing beams in plasmas[3]. The expected luminosity enhancement obtained in this state is calculated in this paper. As understanding the approach to this equilibrium entails examining nonlinear phase space dynamics, approximations are necessary, especially with regards to the calculation of the emittance growth induced by filamentation. A model for this emittance growth, based partially on O. Anderson's methods which were introduced for the study of the theory of space charge induced emittance growth[4], is employed, which then allows a calculation of luminosity enhancement factors that is in excellent agreement with the values obtained by simulation.

The equilibrium states we are presently examining are of the type known as Maxwell-Vlasov equilibria, which are obtained by looking for a time independent solution of the Vlasov equation describing the beam's transverse phase space, with the forces obtained self-consistently from the Maxwell equations using the beam charge and current profiles. We begin by analyzing a limiting case, that of a flat, or sheet, beam ($\sigma_x \gg \sigma_y$), as these are the simplest, and most likely to be found at the interaction point

of a linear collider. For the purpose of calculation and comparison to simulations[1] the beams are assumed to be uniform in x and z (at least locally), and have identical profiles in y . In this way, the model of an equilibrium state can be constructed.

II. Maxwell-Vlasov Equilibria

In order to describe a thermally equilibrated, self-pinchd state of the beam, we begin by writing the vertical force on an ultra-relativistic particle due to the electric and magnetic fields of the opposing beam as

$$F_y(y) = (1 + \beta^2)qE_y \cong 2qE_y = -8\pi e^2 \Sigma_b \int_0^y Y(y') dy', \quad (2)$$

where Y , normalized by $\int_{-\infty}^{\infty} Y(y) dy = 1$, describes the vertical beam spatial distribution function, and $\Sigma_b = N/2\pi\sigma_x\sigma_z$ is the sheet beam surface charge density. We search for separable solutions to the time independent Vlasov equation

$$v_y \frac{\partial f}{\partial y} = -F_y \frac{\partial f}{\partial p_y}, \quad (3)$$

where $v_y = p_y/\gamma m$, *i.e.* solutions of the form $f(y, p_y) = Y(y)P(p_y)$. This form is in fact approached in true thermal equilibrium, as can be verified by substitution of a Maxwellian momentum distribution, and this is illustrated below. In order for this equilibrium to be approached through phase space mixing, more than one nonlinear vertical betatron oscillation must occur during collision, $D_y \cong 4\pi r_e \Sigma_b \sigma_z^2 / \sigma_y > 2\pi$. [3][5].

The solution to the momentum equation

$$\frac{dP}{dp_y} = -\frac{\lambda^2}{\gamma m} p_y P(p_y) \quad (4)$$

derived from separation of Eq. (3) is

$$P(p_y) = \frac{\lambda}{\sqrt{2\pi\gamma m}} \exp\left(-\frac{\lambda^2 p_y^2}{2\gamma m}\right) \quad (5)$$

which is the Maxwell-Boltzmann form corresponding to a thermal equilibrium. The separation constant $\lambda^2 = \gamma m / \sigma_p^2$, with $\sigma_p^2 = \langle p^2 \rangle$, is inversely proportional to the temperature of the system. The solution to the corresponding coordinate equation

$$\frac{dY}{dy} = -8\pi e^2 \lambda^2 \Sigma_b Y(y) \int_0^y Y(\xi) d\xi \quad (6)$$

derived from Eq. (3) is

$$Y(y) = \frac{\alpha}{2} \operatorname{sech}^2(\alpha y), \quad \alpha = 4\pi e^2 \Sigma_b \lambda^2. \quad (7)$$

This profile is the one-dimensional analogue to the Bennett profile found in a cylindrically symmetric Maxwell-Vlasov equilibrium[2-3].

The separation constant λ^2 still remains to be calculated in this treatment. To obtain an initial estimate, one can use the fact that the distribution function at the origin in phase space is stationary, by symmetry, that is $\partial f / \partial t = 0$ at $(y, p_y) = (0, 0)$, and therefore $f(0, 0)$ is a constant of the motion. Assuming an initial bi-gaussian distribution in phase space, and equating its peak density in phase space to that of the Bennett-type profile found upon equilibration, we have

$$f(0, 0) = Y(0)P(0) = \frac{1}{2\pi \epsilon_n m c} = \sqrt{\frac{2\pi}{\gamma m}} \lambda^3 e^2 \Sigma_b \quad (8)$$

We then obtain, solving directly for α ,

$$\alpha = \left[\frac{8\gamma \epsilon_n \Sigma_b}{\epsilon_n^2} \right]^{1/3} \quad (9)$$

With this relation we can now compare the luminosity that comes about by the transition to a pinch confined Bennett-like state with that of the initial unpinched Gaussian beam. At this point, we make allowance for the fact that the beams are not uniform in z and redefine, for the purpose of luminosity calculation, the surface charge density to be its rms value

$$\Sigma_b \rightarrow \langle \Sigma_b^2 \rangle^{1/2} = \frac{N}{\sqrt{8\pi\sigma_x\sigma_z}}. \quad (10)$$

The luminosity enhancement due to pinch-confinement can be calculated by evaluating the luminosity integrals of the two cases, assuming $A_{x,y} \equiv \sigma_z / \beta_{x,y}^* < 1$, where $\beta_{x,y}^* = \sigma_{x,y}^2 / \varepsilon_{x,y}$ are the depth of foci in the transverse dimensions in the interaction region, and $D_x < 1$. In these limits the pinching in the horizontal dimension is negligible, and the effects of transverse beam size variations in the absence of disruption can be ignored. If the disruption is ignored, the luminosity is given by

$$\mathcal{L} = f_{rep} c \int_{-\infty}^{\infty} \int_{-\infty}^{\infty} \int_{-\infty}^{\infty} n_e(x, y, z - ct) n_e(x, y, z + ct) dx dy dz dt = \frac{N^2 f_{rep}}{4\pi\sigma_x\sigma_y}, \quad (11)$$

where f_{rep} is the bunch collision rate of the linear collider. For the pinch confined case, the luminosity integral becomes

$$\mathcal{L} = \frac{N^2 f_{rep} \alpha}{6\sqrt{\pi\sigma_x}}. \quad (12)$$

The luminosity enhancement factor, which is defined to be the ratio of the luminosity of the pinch confined collisions to the undisturbed case, is, from Eqs. 11 and 12,

$$H(D_y, A_y) = \frac{4\sqrt{\pi}\sigma_y}{3} \left[\frac{\gamma^3 r_c \Sigma_b}{\varepsilon_y^2} \right]^{1/3} = \frac{2}{3} \left[\frac{\sqrt{2\pi} D_y}{A_y^2} \right]^{1/3} \quad (13)$$

This results of the computer simulation of luminosity enhancement factors by Chen and Yokoya[1] is reprinted in Figure 1. Equation 13 clearly has too strong a dependence on both D_y and A_y to model the simulation results correctly. This is because, even though we have invoked emittance growth (phase space filamentation) as the mechanism behind collisionless approach to equilibrium, we have neglected to calculate this emittance growth. In other words, the filamented phase space may produce behavior like that of a smooth thermal distribution function, but since it is filamented, the relationship between the peak in the distribution function and the emittance is no longer simply given by Eq. 8, and our calculation is too optimistic.

III. Emittance Growth

Assuming the vertical disruption is large, the emittance growth occurs during two distinct times during the approach to pinch confinement. The first is a "wave-breaking" in phase space, where the nearly laminar initial focusing process ends with the advent of focusing to the y -axis of the small amplitude beam particles. This is very similar the space-charge induced emittance growth in low energy focusing channels, and is analyzed with a method developed in that field by Anderson[4]. We begin by assuming laminar flow of beam particles pinching down under the influence of the opposing beam forces. This assumption ignores the effects of the beams' finite emittance. In addition, the opposing beam is assumed to be undergoing an identical pinch, reducing the model problem to that of calculating the behavior of a single beam. In order to recover the relevant aspects of the time dependence of the initial pinching forces, we assume that the opposing beam current, and therefore the pinching forces, rise linearly in time, as $b_1 ct / \sigma_z$, where b_1 is a constant of order unity introduced to account for the uncertainty in the rise time. The force on the beam particles in this region of rising beam current can then be written in terms of the enclosed opposing beam current, and thus the initial transverse displacement $\xi \equiv y(t=0)$

$$F_y = 8\pi e^2 \Sigma_b G(\xi) b_1 \frac{z}{\sigma_z}, \quad (14)$$

where $G(\xi) = \int_0^\xi Y(y) dy$ is a constant of the motion under the assumed double laminar flow conditions. The equation of motion for the beam particles is then

$$y'' + K(\xi) b_1 \frac{z}{\sigma_z} = 0, \quad ' \equiv \frac{d}{dz}, \quad (15)$$

with $K(\xi) = 8\pi r_e \Sigma_b G(\xi) / \gamma$. For small initial amplitudes $\xi \ll \sigma_y$ we have

$$K(\xi) \equiv \frac{8\pi r_e n_e}{\gamma} \xi \equiv k_\beta^2 \xi \quad (16)$$

where $n_e = \Sigma_b / \sqrt{2\pi} \sigma_y$ is the peak undisturbed beam density, and we have defined the wave-number associated with vertical betatron motion associated with the forces arising

from an oncoming beam of this density. The solution for the small amplitude limit of Eq. 15 is thus

$$y = \xi \left[1 - \frac{b_1 k_\beta^2 z^3}{6 \sigma_z} \right] \quad (17)$$

and the small amplitude particles focus at the wave-breaking point $z_{wb} = \left[6 \sigma_z / b_1 k_\beta^2 \right]^{1/3}$.

The general solution to Eq. 15 is

$$y = \xi \left[1 - \frac{b_1 k_\beta^2}{6 \sigma_z} \frac{G(\xi)}{\left. \frac{dG}{d\xi} \right|_{\xi=0}} z^3 \right] \quad (18)$$

At wave-breaking, which corresponds to one-quarter of a beam oscillation, and after which the laminar flow assumption is violated, the particle positions have dependence which has no term linear in ξ , which is an indication of the explosive emittance growth which has taken place.

The growth of the square of the rms emittance at wave breaking can be calculated by substitution of particle positions and angles at z_{wb} into the following expression

$$\Delta \epsilon_y^2 = \left[\langle y^2 \rangle \langle y'^2 \rangle - \langle yy' \rangle^2 \right]_{z=z_{wb}} = b_2 \frac{\sigma_y^4}{\sigma_z^2} D_y^{2/3}, \quad (19)$$

where b_2 is a constant dependent only on b_1 and on the exact form of G . The total emittance at wave-breaking is therefore, adding the initial thermal and the nonlinear contributions in squares, and using $\sigma_y = \sqrt{\beta_y^* \epsilon_{y,0}}$, is given by

$$\epsilon_{y,z_{wb}}^2 = \epsilon_{y,0}^2 \left[1 + b_2 \frac{D_y^{2/3}}{A_y^2} \right]. \quad (20)$$

This would complete the description of the relevant emittance growth if the applied forces had no further time dependence, as the emittance, and thus the peak beam density and differential luminosity, quickly equilibrates after wave-breaking in a system

with constant current[3]. Because the beam-beam forces must still undergo further increase, however, there is more emittance growth due to the induced turbulence in the beams' transverse phase space as the nearly equilibrated beam pinches further under a nonlinear restoring force. This has some analogy to the emittance growth in a space-charge dominated focusing channel discussed recently by Bohn[6]. The phase-space turbulence which occurs after wave-breaking, combined with the nonlinearity and the time ramp of the pinching forces, cause an emittance growth. This growth is not well quantified by the rms emittance, since that would overemphasize the contribution of the tails of the phase space. What we are concerned with here is actually the phase space density in the *vicinity* of the origin, as that is what dictates the equilibrium beam density profile and therefore the differential luminosity. As the dilution of the peak phase space density occurs during turbulence, the motion displays some aspects of chaotic behavior. In particular, we can expect that two nearby points in phase space will diverge exponentially from each other (with a characteristic Lyapunov exponent) as the motion proceeds, leading to an exponential increase in effective phase space area, or emittance.

This observation allows us to construct a simple model with which to quantify the effective emittance growth. The fractional rate of increase of the phase space area (the emittance ε_y) must be proportional to the inverse of the current rise length σ_z^{-1} (how fast the wave-number of the focusing ramps as the beams come into collision) and also proportional to the phase space mixing angle occurring during a rise length, $k_\beta \sigma_z \approx \sigma_z / \beta_y^*$. Note that by taking $k_\beta \approx \beta_y^{*-1}$, a constant, we have only supplied an estimate of the thermalization length. This estimate is quite good because the thermal spread of the filaments of the distribution will have nearly the same effective temperature as the original, unpinched phase space, because of the nonlinearity of the pinching forces. Under these assumptions, a soluble approximate equation describing the emittance growth after wave-breaking can be written,

$$\frac{d\varepsilon_y}{dz} \approx b_3 \frac{\varepsilon_y}{\beta_y^*}, \quad (21)$$

where b_3 is a constant of order unity which contains information about rise length and the amplitude of the nonlinear terms in the pinch forces. As we expect the density to be well behaved near $y=0$, the dominant nonlinearity is the lowest term, of third order in ζ . Integrating Eq. 21 over the entire current ramp (it is easy to show that for $D_y \gg 1$, the wave-breaking distance may be ignored $z_{wb} \ll \sigma_z$) gives, in combination with Eq. 20, the final effective emittance at the end of the ramp

$$\varepsilon_{y,\sigma_z}^2 = \varepsilon_{y,0}^2 \left[1 + b_2 \frac{D_y^{2/3}}{A_y^2} \exp(2b_3 A_y) \right]. \quad (22)$$

Now there are two constants that must be determined in order to derive the full expression for the luminosity enhancement. Using these constants as fitting parameters to model the simulation data, we obtain a final expression for the emittance growth

$$\varepsilon_{y,\sigma_z}^2 = \varepsilon_{y,0}^2 \left[1 + \frac{1}{9} \frac{D_y^{2/3}}{A_y^2} \exp\left(\frac{\pi}{6} A_y\right) \right]. \quad (23)$$

and the luminosity enhancement as

$$H(D_y, A_y) = \frac{2}{3} \left[\frac{\sqrt{2\pi} D_y}{A_y^2 + \frac{1}{9} D_y^{2/3} \exp\left(\frac{\pi}{6} A_y\right)} \right]^{1/3}. \quad (24)$$

The fit to the simulation data obtained from Eq. 24 is shown in Figure 1, and as can be seen, it is quite good. The standard deviation of the error between the data and the fit is 1.2 percent over the ranges $A_y = \{0.1, 0.8\}$ and $D_y = \{10, 100\}$, while the maximum error is 2.5 percent. This agreement lends strong support for the validity of the model we have developed for the pinch-confined state observed in the simulations[1].

IV. Round Beam Equilibria and Luminosity Enhancement

While the disruption enhancement occurring in round beam ($\sigma_x^* = \sigma_y^*$) collisions is not of as great interest as for flat beams, due to the emphasis of current linear collider designs on flat beam collisions (which mitigate the coherent production of photons and associated problems), it has been investigated thoroughly in the last decade, mainly motivated by the need to understand the original SLC design and operation. One curious fact which has emerged from the comparison of round versus flat beam collisions is that the luminosity enhancement appears to scale as

$$H(D, A)_{round} \equiv H(D_y, A_y)_{flat}^3. \quad (25)$$

It is interesting to see what a Maxwell-Vlasov analysis predicts as far as explaining this scaling is concerned. While the full discussion of the emittance growth process for the disruption of round beams[5] is beyond the scope of the present work, we will see below that the results of such a calculation would yield similar dependences on D and A as in the flat beam case. This said, we can follow the treatment of self-focused round beam equilibria in plasma found in Ref. 2, to derive the analogue to Eq. 13 for cylindrical symmetry. We begin by writing the Vlasov equation for this case

$$\frac{p_r}{\gamma m} \frac{\partial f}{\partial r} = -F_r \frac{\partial f}{\partial p_r} \quad (26)$$

Assuming separable solutions, $f(r, p_r) = R(r)P(p_r)$, the momentum equation and its solution are of identical form to Eqs. 4 and 5. The corresponding coordinate equation is

$$\frac{dR}{dr} = -R \left(\frac{4e^2 \lambda^2 N_b}{r} \right) \int_0^r R(\rho) \rho d\rho, \quad (27)$$

where N_b is the number of beam particles per unit length. The solution of Eq. 27 is the well-known Bennett profile

$$R(r) = \frac{1}{\pi a^2 \left[1 + (r/a)^2 \right]^2}, \quad (28)$$

where $a^2 = 2\gamma \epsilon_r^2 / N_b r_c$, and we again take the rms value of the longitudinal charge density N_b .

The luminosity enhancement obtained in this case (leaving the phase space dilution term $\epsilon_r / \epsilon_{r,0}$ unspecified for the moment), repeating the method used in deriving Eq. 13, is

$$H(D, A)_{\text{round}} = \frac{4\sigma_r^2}{3a^2} = \left[\frac{2D}{3A^2} \right] \left(\frac{\epsilon_{r,0}}{\epsilon_r} \right)^2 \quad (29)$$

Comparison of this expression to Eqs. 13 and 24 indeed indicates that $H(D, A)_{\text{round}} \approx H(D_y, A_y)_{\text{flat}}^3$, as found by simulation.

To illustrate this point further, we compare the simulation data to an expression of the same form as Eq. 23, adjusting the constants and the dependence on D of the emittance growth to obtain a best fit to the data, to obtain

$$H(D, A) = \frac{2}{3} \left[\frac{D}{A^2 + \frac{1}{10} D^{0.7} \exp(\frac{\pi}{2} A)} \right]. \quad (30)$$

The simulation data and the predictions of Eq. 30 are shown in Fig. 2. Again, the agreement is quite good, with an rms error which is larger than the corresponding flat beam error by approximately three, as might be expected from the ratio of the powers of the functional dependences in the two cases.

Two aspects the emittance growth physics in round beams can be deduced from the fit obtained from Eq. 30. The first is that the D dependence of the emittance growth is slightly stronger for round beams. This is due to the fact that the time dependence of the beam-beam pinching force is stronger than the current rise (the dependence assumed in Eq. 14) in the round beam case. For round beams the force, again assuming laminar flow, is proportional to the enclosed current, but it is also inversely proportional to the radius of the particle undergoing the pinch, which obviously becomes smaller during the pinch.

The other notable feature implied by Eq. 30 is that the exponent for the emittance growth due to phase space dilution after initial wave-breaking is a factor of three larger than found in the flat beam case. This factor is present because of the same geometric factors relating current density and pinching forces which produce the difference in exponents in Eq. 25, and is a measure of the coefficient of the nonlinear focusing term producing the phase space dilution. To illustrate this point, we expand the focusing forces corresponding to the flat beam

$$F_y \cong -8\pi e^2 n_b y \left[1 - \frac{1}{3} \left(\frac{y}{a_y} \right)^2 \right], \quad (31)$$

where $a_y \equiv \alpha^{-1}$, and round beam

$$F_r \cong -4\pi e^2 n_b r \left[1 - \left(\frac{r}{a} \right)^2 \right] \quad (32)$$

equilibria. The quantities a_y and a are related to the thermal scale (Debye) lengths which indicate the distances over which the spatial distributions fall off quadratically from their peak value in the flat and round beam equilibria, respectively. Expanding the equilibrium profiles for small amplitude, we have

$$n_b \equiv \begin{cases} n_b(0) \left[1 - \left(\frac{y}{a_y} \right)^2 \right] & \text{flat beams,} \\ n_b(0) \left[1 - 2 \left(\frac{r}{a} \right)^2 \right] & \text{round beams.} \end{cases} \quad (33).$$

We can see that, by defining the beam boundary in terms of its quadratic density variations, $a/\sqrt{2}$ is equivalent to a_y . Now, the phase space dilution rate is proportional to the relative difference in the betatron tune with amplitude, which is linearly dependent on the coefficient of third order focusing terms[7] in Eqs. 31 and 32. Thus the e-folding distance for the emittance growth, taking into account the relationship between the beam boundaries, should be approximately a factor of 3/2 larger in the round beam case. When the emittance growth term is squared, this produces the factor of three difference in the exponents found in Eqs. 24 and 30 for the growth of ε^2 .

V. Conclusions

This approach to understanding beam-beam collisions can be used to perform more accurate estimations of radiative (beamstrahlung) energy losses, and the differential luminosity spectrum[8]. In addition, a good physical model for the distribution functions of the beams as they undergo collision is a necessary starting point for an improved analysis of the transverse instabilities[1][9] (especially the kink instability) of the colliding beam system. An analogous investigation of the transverse two-stream instabilities of slab beams in overdense plasmas has been recently performed by Whittum[10]. His methods may be straightforwardly adopted for analyzing the beam-beam kink instability. The methods introduced here will also be extended to the study of quasi-flat beam collisions[11], where the horizontal disruption may be non-trivial, in a future work.

In conclusion, we have introduced a model of the luminosity enhancement due to beam-beam disruption in a linear collider by examining the transverse equilibria (the pinch-confined states observed in simulation) which are approached collisionlessly through phase space mixing in the limit of large disruption. Simple aspects of the nonlinear dynamics involved have been employed to obtain the scaling, as a function of the disruption parameter D and thermal factor A , of pinch confined beam densities and luminosity enhancements. This model gives quantitatively very good agreement with computational simulations, and explains some important details of the relationship between round and flat beam luminosity disruption enhancement observed in these simulations.

References

1. P. Chen and K. Yokoya, *Phys. Rev. D* **38**, 987 (1988) and K. Yokoya and P. Chen, in *Frontiers of Particle Beams: Intensity Limitations*, Lecture Notes in Physics **400** (Springer-Verlag, Berlin, 1992).
2. W. H. Bennett, *Phys. Rev.* **45**, 890 (1934), and *Phys. Rev.* **98**, 1584 (1955).
3. J. B. Rosenzweig, P. Schoessow, B. Cole, W. Gai, C. Ho, R. Konecny, S. Mtingwa, J. Norem, M. Rosing, and J. Simpson, *Phys. Fluids B* **2**, 1376 (1990).
4. O.A. Anderson, *Particle Accelerators* **21**, 197 (1987).
5. Model calculations of emittance growth using particle-in-cell simulations have been performed by W. Mori, T. Katsouleas and J.J. Su, *Particle Accelerators* **31**, 21 (1990).
6. C.L. Bohn, *Phys. Rev. Lett.* **70**, 932 (1993).
7. G. Dome, CERN Report 84-15 (Geneva, 1984).
8. P. Chen, in the *Proceedings of the 1991 Particle Accelerator Conference* **5**, 3255 (IEEE, 1991), also P. Chen, *Phys. Rev. D* **46**, 1186 (1992).
9. J. B. Rosenzweig, B. Autin and P. Chen, in the *Proceedings of the 1989 Lake Arrowhead Workshop on Advanced Accelerator Concepts*, 324 (AIP, New York, 1989).
10. D.H. Whittum, *Phys. Fluids B* **5**, 4432 (1993).
11. P. Chen, in the *Proceedings of the 1993 Particle Accelerator Conference* **1**, 617 (IEEE, 1993).

Figure Captions

Figure 1. The results of particle-in-cell simulation (plotted symbols) of luminosity enhancement in flat beam collisions, taken from Ref. 1, along with fit obtained by Maxwell-Vlasov equilibrium analysis derived expression, Eq. 24.

Figure 2. The results of particle-in-cell simulation (plotted symbols) of luminosity enhancement in round beam collisions, taken from Ref. 1, along with fit obtained by Maxwell-Vlasov equilibrium analysis derived expression, Eq. 30.

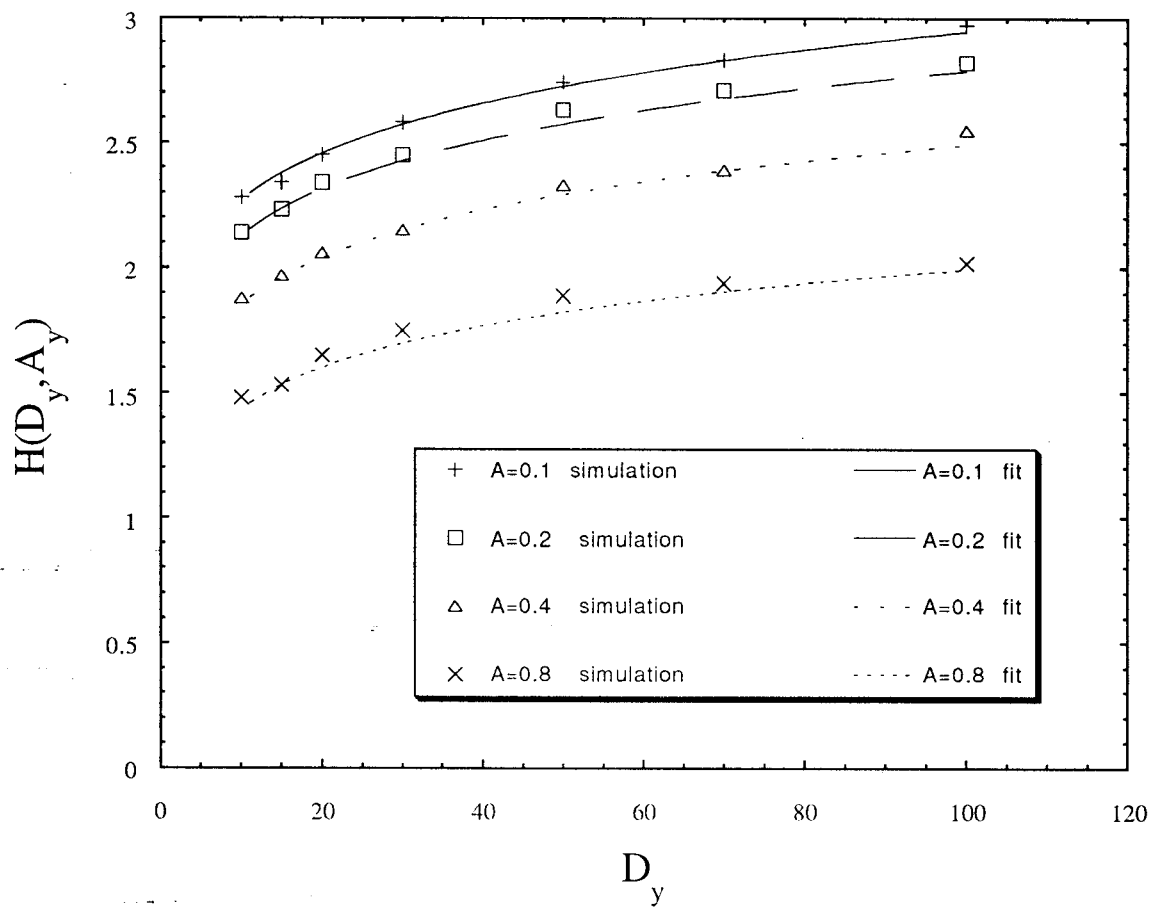


Figure 1

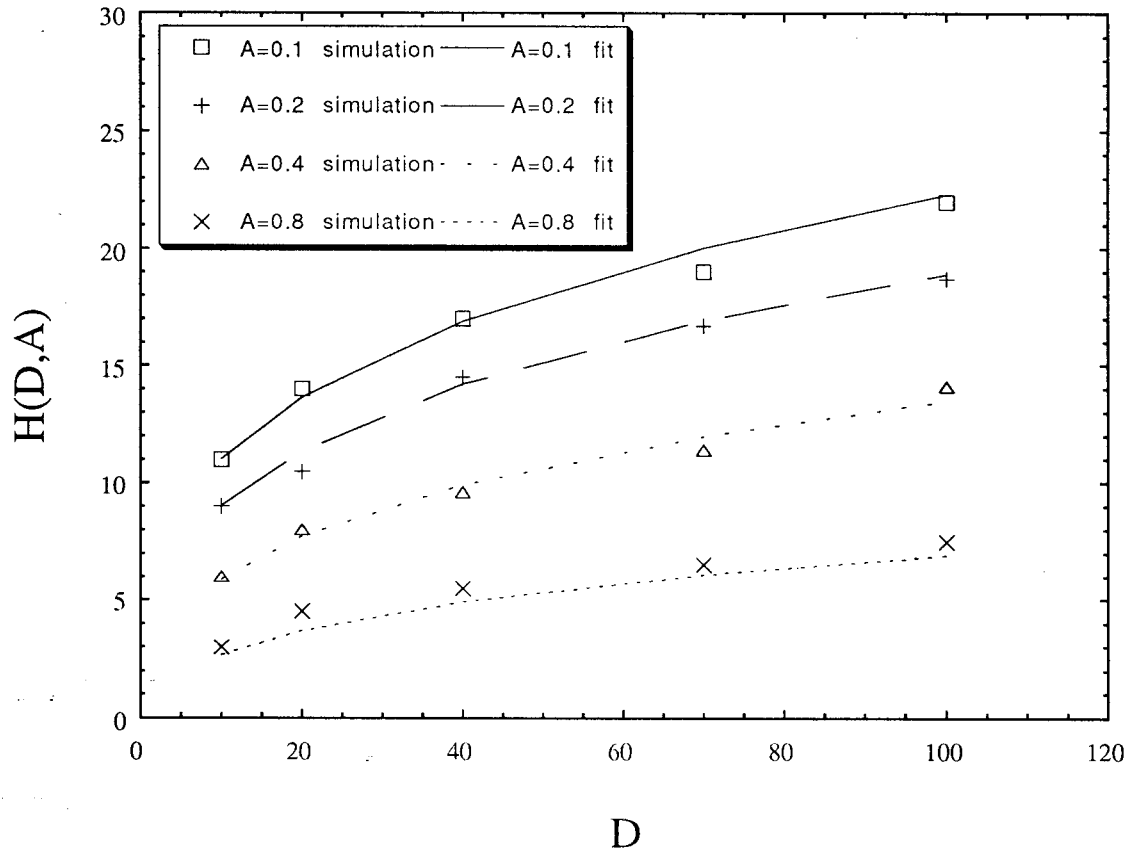


Figure 2